The Journal of Immunology

Clustering of Class I HLA Oligomers with CD8 and TCR: Three-Dimensional Models Based on Fluorescence Resonance Energy Transfer and Crystallographic Data

Rezso Gáspár, Jr., Péter Bagossi, László Bene, János Matkó, János Szöllosi, József Tozsér, László Fésüs, Thomas A. Waldmann and Sándor Damjanovich

J Immunol 2001; 166:5078-5086; ;
doi: 10.4049/jimmunol.166.8.5078
http://www.jimmunol.org/content/166/8/5078

The Journal of Immunology is published twice each month by
The American Association of Immunologists, Inc.,
1451 Rockville Pike, Suite 650, Rockville, MD 20852

Print ISSN: 0022-1767 Online ISSN: 1550-6606.

Clustering of Class I HLA Oligomers with CD8 and TCR: Three-Dimensional Models Based on Fluorescence Resonance Energy Transfer and Crystallographic Data[1]

Rezső Gáspár, Jr.,[2]* Péter Bagossi,† László Bene,* János Matkó,* János Szöllősi,* József Tőzsér,† László Fésüs,† Thomas A. Waldmann,§ and Sándor Damjanovich*‡

Fluorescence resonance energy transfer (FRET) data, in accordance with lateral mobility measurements, suggested the existence of class I HLA dimers and oligomers at the surface of live human cells, including the B lymphoblast cell line (JY) used in the present study. Intra- and intermolecular class I HLA epitope distances were measured on JY B cells by FRET using fluorophore-conjugated Ag-binding fragments of mAbs W6/32 and L368 directed against structurally well-characterized heavy and light chain epitopes, respectively. Out-of-plane location of these epitopes relative to the membrane-bound BODIPY-PC (2-(4,4-difluoro-5-(4-phenyl-1,3-butadienyl)-4-bora-3a,4a-diaza-*s*-indacene-3-pentanoyl)-1-hexadecanoyl-*sn*-glycero-3-phosphocholine) was also determined by FRET. Computer-simulated docking of crystallographic structures of class I HLA and epitope-specific Ag-binding fragments, with experimentally determined interepitope and epitope to cell surface distances as constraints, revealed several sterically allowed and FRET-compatible class I HLA dimeric and tetrameric arrangements. Extension of the tetrameric class I HLA model with interacting TCR and CD8 resulted in a model of a supramolecular cluster that may exist physiologically and serve as a functionally significant unit for a network of CD8-HLA-I complexes providing enhanced signaling efficiency even at low MHC-peptide concentrations at the interface of effector and APCs. ***The Journal of Immunology*****, 2001, 166: 5078–5086.**

Class I and class II HLA glycoproteins with bound antigenic peptides are expressed on the surface of APCs and serve as specific ligands for TCRs of cytotoxic and Th lymphocytes, respectively. Although extensively studied in the last decade, some molecular details of the MHC-TCR interaction still remained unresolved and controversial, e.g., it is not clear how many TCRs or MHC-peptide ligands are required to trigger an efficient T cell signaling. Alternative theories were proposed to explain the apparent paradigm of low affinity MHC-TCR interaction vs the observed highly specific and efficient (sustained) T cell activation, such as the conformational change/TCR clustering (1) or the serial triggering (2) hypotheses. Clustering of TCRs was reported as an essential step in induction of efficient activation signals (1–3). The mechanism by which TCRs clusterize, however, is still not clear.

Conflicting data were reported about the critical number of MHC-peptide ligands necessary to trigger T cell activation. Monomers of soluble class I MHC-peptide ligands were shown to trigger calcium responses in CD8$\alpha\beta^+$, but not in CD8$^-$ T cells (4), suggesting that the presence of CD8 coreceptor and its interaction with both TCR and MHC-I molecules are also prerequisite of an efficient T cell activation. In contrast, Boniface et al. (5) reported that only dimers or tetramers, but not the monomer of the soluble murine MHC (IE^k)-peptide ligand could stimulate T cells with a sufficient efficiency. Formation of supramolecular activation clusters in T cells upon Ag stimulus was also found to be dependent on the arrangement of MHC-peptide ligands (3). Thus, the question arises whether a proper supramolecular organization of MHC-peptide ligands on APCs is also critical to an efficient T cell stimulation. While molecular organization of the TCR-related signaling components has extensively been investigated recently, not much attention has been paid to MHC-peptide organization on APCs.

Fluorescence resonance energy transfer (FRET)[3] measurements of molecular proximities on the nanometer scale and lateral diffusion measurements by single particle tracking both can directly probe clustering/association of proteins in the plasma membrane of live cells (6–10). Spontaneous homo-association of class I HLA molecules has been detected earlier in proteoliposomes (11), on activated T and B lymphocytes, and on a number of transformed human cell lines by FRET and long-range electron transfer (12–16). The existence and spatial arrangement of such class I HLA oligomers on APCs may have important functional consequences; therefore, it should also be considered in modeling the MHC-TCR interaction.

X-ray crystallographic structures of HLA molecules and their complexes with peptides (17–20) are sufficiently well resolved and provide detailed three-dimensional (3D) structural information to

Departments of *Biophysics and Cell Biology and †Biochemistry and Molecular Biology, and ‡Biophysics Research Group of the Hungarian Academy of Sciences, University of Debrecen, Medical and Health Science Center, Debrecen, Hungary; and §Metabolism Branch, National Cancer Institute, National Institutes of Health, Bethesda, MD 20892

Received for publication January 21, 2000. Accepted for publication January 23, 2001.

The costs of publication of this article were defrayed in part by the payment of page charges. This article must therefore be hereby marked *advertisement* in accordance with 18 U.S.C. Section 1734 solely to indicate this fact.

[1] This work was supported by Grants OTKA T029947, FKFP 327/2000, and ETT T05/102/2000 (to R.G.); OTKA F020590 and Bolyai Research Fellowship (to L.B.); FKFP 0518/99 (to J.M.); OTKA T019372 and T030399 (to J.S.); and OTKA T023873 and T030411 (to S.D.).

[2] Address correspondence and reprint requests to Dr. Rezső Gáspár, Department of Biophysics and Cell Biology, University of Debrecen, Medical and Health Science Center, P.O. Box 39, 4012 Debrecen, Hungary. E-mail address: gaspar@jaguar.dote.hu

[3] Abbreviations used in this paper: FRET, fluorescence resonance energy transfer; 3D, three-dimensional; β_2m, β_2-microglobulin; BODIPY-PC, 2-(4,4-difluoro-5-(4-phenyl-1,3-butadienyl)-4-bora-3a,4a-diaza-*s*-indacene-3-pentanoyl)-1-hexadecanoyl-*sn*-glycero-3-phosphocholine; Fab, Ag-binding fragment; SFX, 6-(fluorescein-5-carboxamido)hexanoic acid succinimidyl ester; TAMRA-X, 6-(tetramethylrhodamine-5(and -6)-carboxamido)hexanoic acid succinimidyl ester.

0022-1767/01/$02.00

localize Ab binding sites (epitopes) on these molecules. However, they do not allow steric positioning (orientation) of the molecule relative to the plane of the plasma membrane, since the crystals are usually developed from digested extracellular domains of the proteins; therefore, the influence of the missing domains (intramembrane helix and cytoplasmic tail) on their conformation and orientation cannot be taken into account.

In the present work, we outline a new approach of computer modeling based on docking epitope-specific Ag-binding fragments (Fab) of mAbs to high resolution x-ray structures combined with their steric positioning on the basis of experimental results from FRET-based epitope mapping performed on membrane-bound intact HLA-I molecules in live cells. Fitting the x-ray-resolved structures to the in situ FRET distance estimates helped to generate 3D models of the possible supramolecular organization of class I HLA molecules, reflecting close to physiological conditions. These 3D models could also consider possible dimerization/oligomerization of these proteins.

In this study, we show that only a limited group of sterically allowed, computer-generated 3D molecular superstructures could be fitted to the FRET data measured on live cells. These include both dimers and tetramers of class I HLA. Furthermore, we show a model of a possible supramolecular cluster built from these HLA-I oligomers, CD8 and TCR molecules, that is sterically allowed and matches FRET data, as well. The importance of such analysis is accentuated by the existing contradiction of views on the necessity of a monomeric (4) or oligomeric peptide-MHC complex (5) in the course of initiation of efficient signal transduction through the TCR. The presented 3D models can be considered as possible in situ arrangements of supramolecular HLA clusters on APCs, also at the site of APC/T cell interface, since herewith we consider only those cases in which the molecular associations of class I HLA molecules are supported by unambiguous physical measurements at the surface of live cells.

Materials and Methods

Cells

The EBV-transformed JY human B lymphoblast cell line (21) was cultured in RPMI 1640 medium supplemented with 10% FCS in 5% CO_2 atmosphere, at 37°C.

mAbs and Fab preparation

W6/32 (IgG2aκ) mAb with specificity for the heavy chain of class I HLA A,B,C molecules and L368 (IgG1κ) mAb specific for β_2-microglobulin (β_2m) were kindly provided by F. Brodsky (University of California, San Francisco, CA). Fab were prepared from mAbs using a method described earlier (22). Briefly, IgG mAbs were dialyzed with phosphate buffer (100 mM Na_2HPO_4, 150 mM NaCl, 1 mM EDTA, pH 8) and digested with activated papain at 37°C for 10 min. The enzyme activity was terminated by addition of iodoacetamide. The reaction mixture was passed through a Sephadex G-100 superfine column. Collected Fab fractions were further separated from the residual IgG content by passing through a protein A-Sepharose column.

Conjugation of Fab with fluorescent dyes

Aliquots of Fab (at least at 1 mg/ml concentration) were conjugated, as described earlier (15), with 6-(fluorescein-5-carboxamido)hexanoic acid succinimidyl ester (5-SFX; Molecular Probes, Eugene, OR), or 6-(tetramethylrhodamine-5(and -6)-carboxamido)hexanoic acid succinimidyl ester (5(6)-TAMRA-X, SR). The proteins were transferred into a carbonate-bicarbonate buffer at pH 8.3, mixed with 30- to 100-fold molar excess of freshly prepared fluorescent dyes (in DMSO), and incubated for 45–60 min, at room temperature. Unreacted dye molecules were removed by gel filtration through a Sephadex G-25 column. Final Ab concentration and the dye to protein ratio were determined spectrophotometrically (15). In case of SFX and TAMRA-X, the ratio varied between 0.8 and 1.2 dye/Fab. The fluorescently tagged Fab retained their biological activity as supported by the competition with identical, but unlabeled Fabs.

Labeling of cells with fluorescent Fabs

Freshly harvested cells were washed twice in ice-cold PBS (pH 7.4). The cell pellet was suspended in 100 μl of PBS (1×10^7 cells/ml) and incubated with ~10 μg of SFX- or TAMRA-X-conjugated Fabs for 60 min on ice. The excess of Fabs was at least 30-fold above the K_d during the incubation. To avoid possible aggregation of the Fabs, they were air fuged (at $5 \times 10^4 \times g$, for 30 min) before labeling. Staining of cells was checked under fluorescence microscope after the labeling procedure. Special care was taken to keep the cells on ice before FRET analysis to avoid significant protein internalization. The labeled cells were washed with excess of cold PBS and then occasionally fixed with 1% formaldehyde. Data obtained with fixed cells did not differ significantly from those of unfixed, viable cells. The number of binding sites on the cell surface was determined from the mean values of flow cytometric histograms of cells labeled to saturation with SFX-conjugated Fabs. The mean fluorescence intensities were converted to number of binding sites by calibration with fluorescent microbeads (Quantum 25; Flow Cytometry Standards, San Juan, PR).

Labeling of cells with lipid probes

The surface of JY cells was labeled for FRET-based vertical distance measurements by 2-(4,4-difluoro-5-(4-phenyl-1,3-butadienyl)-4-bora-3a,4a-diaza-*s*-indacene-3-pentanoyl)-1-hexadecanoyl-*sn*-glycero-3-phosphocholine (BODIPY-PC (581/591)) as acceptor for SFX-conjugated Fabs bound either to the heavy or the light chain of class I HLA molecules. When labeling with BODIPY-PC (581/591) (Molecular Probes), a final concentration of up to 5 μg/ml of dye was added to the cell suspension, at a cell density of $4–5 \times 10^6$ cells/ml. Labeling was conducted for 20 min on ice, followed by 20 min at 37°C. Cells were washed with ice-cold PBS, labeled with Fabs, and analyzed immediately by flow cytometry. Cells were kept in ice-cold buffer also during the flow cytometric analysis.

Flow cytometric resonance energy transfer measurements

Flow and image cytometric techniques based on FRET, a spectroscopic ruler working on the 2- to 10-nm scale, are very suitable for studying conformation and associations of biomolecules (8, 23–27). Efficiency (probability) of FRET depends on inverse sixth power of the actual separation distance of donor and acceptor dyes (confined in this study to the V domains of Fab molecules). This holds only if the effect of spatial orientation of donor and acceptor dipoles on FRET efficiency can be neglected (27). In our study, the spacer groups on the dyes allowed a reasonable dynamic averaging of dipole orientations, as confirmed by the low value of fluorescence anisotropy of cell-bound dye-Fab conjugates ($r < 0.15$).

In the present study, the FRET efficiency was determined in a Becton Dickinson (Sunnyvale, CA) FACStar^{Plus} flow cytometer, by measuring both the extent of donor-quenching and acceptor sensitization through detecting spectrally selected fluorescence intensities on cell by cell basis, as described in details earlier (25, 26, 28). The efficiency of energy transfer (E) is expressed as percentage of the donor's (SFX) excitation energy tunneled to the acceptor (TAMRA-X) molecules. The mean values of the energy transfer efficiency histograms (determined on a cell population; see Fig. 1*B*) were used and tabulated as characteristic FRET efficiencies between two epitopes. Intra- and intermolecular epitope distances as well as the out-of-membrane plane location of HLA epitopes were determined by FRET, using the strategy shown in Fig. 1*A*.

Determination of distances perpendicular to the cell membrane

In case of protein to lipid FRET measurements, the fluorescent proteins are surrounded by a large array of acceptor-labeled lipids. Therefore, the efficiency of FRET in this study will also depend on the donor to acceptor ratio. In such a situation only, "closest approach distances of labeled epitopes from the membrane surface" (perpendicular to the cell membrane) can be estimated according to the theory and model described by Yguerabide (29, 30). The use of this approach is justified by the observation that at the applied concentrations of the lipid probe the Stern-Volmer plots displaying I_{da}/I_d (ratio of donor intensities in the presence and absence of acceptor, respectively) vs the surface density of BODIPY-PC varied linearly. On the basis of the overlap between absorption and emission spectra of the applied dyes, we used R_o value of 3.9 nm for the SFX-BODIPY PC (581/591) donor-acceptor pair. The calculation of closest distance for Fabs from the cell membrane is described in details in the footnote of Table I.

Molecular modeling

Three-dimensional molecular models were created from the crystal structure of the extracellular domain of HLA-A2 (PDB code: 1AKJ) and that of human Fab B7-15A2 (PDB code: 1AQK). L368-binding epitope was identified by Asp^{38}, Glu^{44}, and Arg^{45} residues of the β_2m of HLA (31, 32), and

Table I. *Intermolecular distances and membrane proximities of Fab bound to β_2m and HLA class I heavy chain measured on JY B lymphoblast cells*

Donor	Determinant	Acceptor	Determinant	$R \pm \Delta R$ (nm)[a]
X-SF-L368	β_2m	TAMRA-X-L368	β_2m	7.9 ± 0.1[b]
X-SF-W6/32	HLA-I heavy chain	TAMRA-X-W6/32	HLA-I heavy chain	7.6 ± 0.1
X-SF-L368	β_2m	TAMRA-X-W6/32	HLA-I heavy chain	6.8 ± 0.1
X-SF-L368	β_2m	BODIPY-PC (581/591)	Membrane surface	7.5 ± 0.2
X-SF-W6/32	HLA-I heavy chain	BODIPY-PC (581/591)	Membrane surface	6.2 ± 0.2

[a] Data represent mean ± SEM values of four independent measurements.

[b] Intermolecular distances (R) were calculated using the inverse-sixth-power distance-dependence law of energy transfer efficiency (E) as follows: $R=R_0N_A^{1/6}(1/E-1)^{1/6}$ with a value of 5.85 nm for the R_0 Förster critical distance of the X-SF-TAMRA-X donor-acceptor pair, and with labeling ratios N_A of 1.3 and 1.2 for the TAMRA-X-labeled L368 and W6/32 Fabs, respectively. The distance errors (ΔR) were derived from energy transfer efficiency errors (ΔE) using the Gaussian error propagation law.

[c] In those cases when the cell membrane was labeled with BODIPY-PC as acceptor, the R values, representing distances of closest approach, were computed from the slopes of straight lines fitted to the experimental Stern-Volmer plots of Fig. 1*C*. In these curves, the fractional change in donor intensity, defined as $E/(1-E) = I_D/I_{DA} - 1$, with E the energy transfer efficiency and I_D and I_{DA} the donor intensities in the absence and presence of acceptor, respectively, was plotted against the surface density of BODIPY-PC. The slopes of the fitting straight lines give the K_q quenching constants, from which the distances of closest approach $R=R_0^{3/2}(\pi/2K_q)^{1/4}$ were computed (29, 30). A value of 3.9 nm was used for the R_0 Förster critical distance based on the emission and absorption spectra of X-SF and BODIPY-PC (581/591), respectively. The surface density of BODIPY-PC was calculated from the applied dye and cell concentrations assuming a total dye uptake by the outer leaflet of the cell membrane. In these calculations a 25-μm cell diameter was used as assessed by flow cytometric forward angle light scattering measurements and calibration with microbeads of known size.

W6/32-binding epitope was identified by Asp^{86} and Lys^{121} residues of the heavy chain of HLA, close to the junction of the peptide-binding domains and also to the β_2m domain (31, 33).

An automated search sequence (using Fortran programs written by one of the authors, P. B.) has been generated to find all possible positions of the Fabs relative to the HLA class I complex in their multimolecular complex corresponding to the situation when fluorescence-labeled Fabs are bound to both the W6/32 and L368 epitopes of the HLA class I molecule (Fig. 2, *A* and *B*). During the process, grid points were assigned to specific locations within the molecules (Fig. 2, *C* and *D*). Fabs were docked into place by the geometrical center of the surface residues of their hypervariable regions (Fig. 2*D*) using a 0.6-nm lower and 1.6-nm upper limits for distances measured from α carbons of the epitope-building residues of HLA (Fig. 2*C*). The lower and upper limits may mimic the contact distances of α carbons of the interacting residues in case of small residue-small residue and bulky residue-bulky residue contacts, respectively. Fluorescent labels on the Fab molecules were found to be confined specifically to the V region of the Fabs (unpublished result: J. T.). FRET-measured interepitope and epitope-to-cell surface distances represent dynamically averaged values based on a cylindrical fluorescence distribution model of fluorescence-labeled cell surface-bound Fab molecules (34). Accordingly, intermolecular distances were estimated in the present study always from the geometrical center of the V region of the Fab molecules (Fig. 2*D*).

Grid points around the HLA molecule were scanned with 0.2-nm steps (corresponding to the accuracy of FRET measurements), and a 1.8-nm-thick region was found as a possible vertical localization of the HLA molecules above the plane of the membrane (XY) based on the FRET-measured interepitope and epitope-to-cell surface distances (the lowest (red) and the highest (cyan) position are shown in Fig. 2*E*).

This layer was searched for possible dimer configurations using as criteria the FRET-measured W6/32-W6/32 and L368-L368 intermolecular distances. The first molecule was allowed to move only in direction of *z*-axis in the layer, while the second molecule was positioned along the Z and Y axes with 0.2-nm steps, and rotation around its axis perpendicular to the membrane was allowed in the range of 0–360 degrees with 15-degree steps. Vertical tilting of the class I HLA molecules was adjusted to position the presented peptide close to parallel to the membrane surface to provide maximal exposure toward the surrounding environment. Top view of the HLA molecules situated in the most populated vertical layer found in this search is shown in Fig. 2*F*. This figure visualizes the effect of the errors originated from the uncertainty of FRET measurements and from the modeling procedure on the accuracy of the in plane (parallel to the cell membrane) position determination of the second HLA molecule compared with a fixed one. Based on this procedure, the allowed distance range between the two HLA molecules is 7–9.4 nm, and for the rotational angle of second molecule −30 to +45 degrees.

The HLA dimer of Fig. 3, *A* and *B*, is one representative example from the closely situated dimeric configurations in Fig. 2*F*. The intermolecular epitope distances correspond to the FRET-determined experimental distance data in Table I and represent a situation when the binding of fluorescent labeled is allowed to both the L368 and W6/32 epitopes. The closely associated dimer of Fig. 3, *C* and *D*, was created by superimposing the membrane-proximal domain of HLA class I on the membrane-proximal domain of the crystal structure of the dimer of HLA class II heterodimers (PDB code: 1SEB). The best fit among the two molecules resulted in 0.16-nm root mean square deviation for the 76–76 α carbon atoms of the respective domains of the molecules. The tetrameric arrangement of Fig. 3, *E* and *F*, was created by superimposing class I HLA-A2 monomers from both kinds of dimers (Fig. 3, *A*, *B*, and *C*, *D*).

A single HLA-A2/peptide/CD8$\alpha\alpha$/TCR complex was created from the crystal structure of HLA-A2/peptide/CD8$\alpha\alpha$ complex (PDB code: 1AKJ) and the crystal structure of HLA-A2/peptide/TCR complex (PDB code: 1AO7) by superimposing the respective HLA molecules. Positions of the HLA molecules in the tetramer of Fig. 3, *G* and *H*, are the same as those of the HLA molecules in the tetrameric complex of Fig. 3, *E* and *F*. Superposition of the structures was performed by using Whatif 4.0 (G. Vriend, EMBL, Heidelberg, Germany) or O 5.8.1 (T. A. Jones, Department of Molecular Biology, Biomedical Centre, Uppsala, Sweden) programs, and the alignments of sequences were created in Clustalw 1.7 (35). Molecular structures were examined on a Silicon Graphics Indigo2 computer running the program Sybyl version 6.3 (Tripos, St. Louis, MO).

The above outlined modeling approach was chosen because the exact primary sequences of the W6/32 and L368 Abs are yet unknown; therefore, traditional force field-based methods could not be used for the optimization of the 3D configuration of the multimolecular complexes investigated.

Results

Estimation of intra- and intermolecular epitope distances of class I HLA molecules on JY B cells by FRET measurements

Fig. 1*A* illustrates the strategy of FRET measurements conducted on JY B cells by the flow cytometric energy transfer method (25, 26). The JY cells are EBV-transformed B lymphocytes (HLA-A2, B7, DR4, DQw1.3)$^+$ (21) with a dominance of the HLA-A2 allelic determinant. Heavy and light chain (β_2m) epitopes on class I HLA molecules were targeted by Fab of W6/32 and L368 mAbs, respectively. The W6/32 Ab was reported to bind near to the Asp^{86} and Lys^{121} residue of the α-chain of HLA class I molecule, close to the junction of the peptide-binding α_1/α_2 domains and also to the membrane-proximal α_3 and β_2m domains (31). Gln^2 of β_2m at the N-terminal region was predicted to be involved in the binding of W6/32 Fab in our computer modeling, due to the close proximity of it to the epitope on the α-chain (33). The antigenic epitope defined by L368 mAb is localized on the human β_2m molecule involving residues Asp^{38}, Glu^{44}, and Arg^{45} of the three-stranded β-pleated sheet of β_2m (31, 32).

For FRET measurements, these Fab were conjugated with either succinimidyl-fluorescein (X-SF) dye, serving as energy donor, or succinimidyl-rhodamine (X-SR) dye, serving as energy acceptor. In average, Fab molecules carried 1 fluorophore/molecule with a high degree of motional freedom (indicated by emission anisotropy values, data not shown) allowing a dynamic orientational averaging (36). This condition allows a reasonable distance estimation from FRET efficiencies, since the statistical average of the

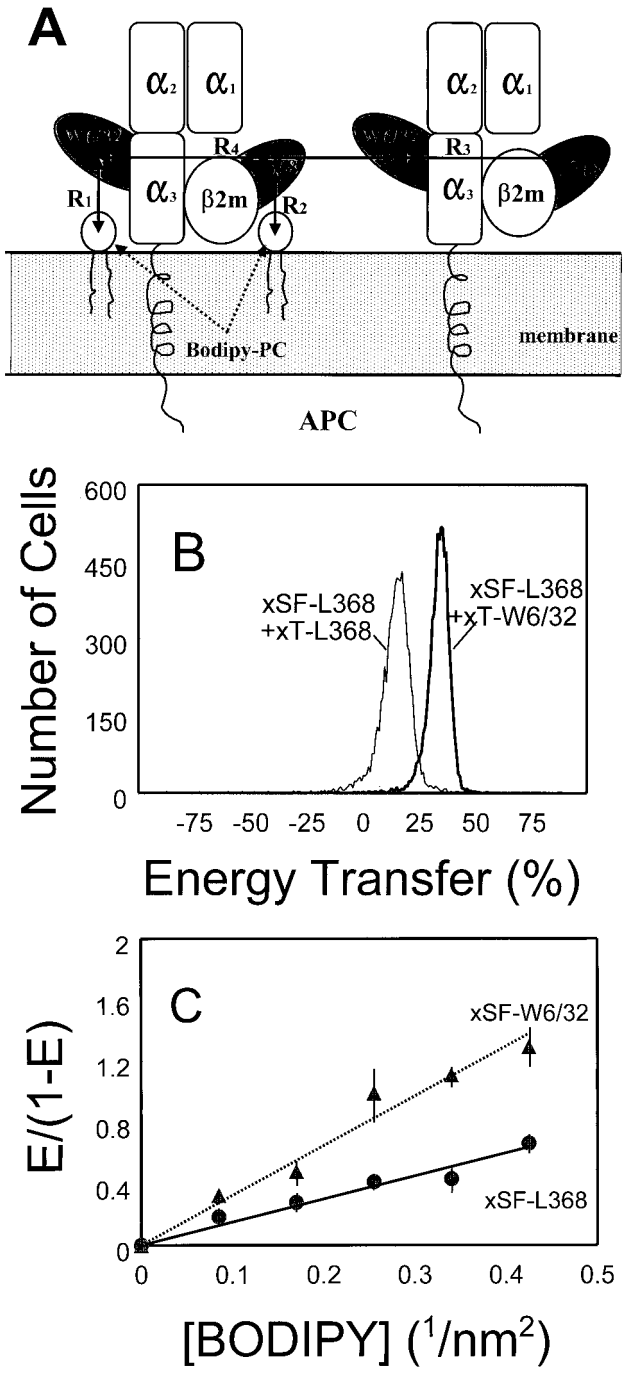

FIGURE 1. Lateral and vertical mapping of class I HLA epitope proximities at the surface of JY human B lymphoblast cells by FRET. *A*, Strategy of FRET measurements on cells. Fab of W6/32 and L368 mAbs conjugated with single X-SF (donor) or TAMRA-X (acceptor) dyes and phosphatidylcholine conjugated with BODIPY/581 (acceptor) were used in the process of monitoring epitope distances from each other and the membrane surface, respectively. Intramolecular distances between heavy and light chain epitopes (R_3), intermolecular distances between two neighboring heavy chains (R_4), between two neighboring light chains (not indicated), as well as vertical distances of these epitopes from the membrane surface (R_1 and R_2) were calculated from FRET efficiencies, as described in *Materials and Methods*. *B*, Representative FRET efficiency histograms displaying FRET efficiency distributions measured between the light chain and heavy chain epitopes of class I HLA (intramolecular FRET, *right histogram*) and between two HLA-I light chains (intermolecular FRET, *left histogram*). *C*, Stern-Volmer presentation of FRET from the heavy chain (●) and light chain (▲) epitopes of HLA-I to the cell surface lipid probe BODIPY-PC. The extent of FRET is displayed as a function of surface density of the acceptor-conjugated phospholipid.

orientation factor (otherwise also influencing FRET efficiency), $\kappa^2 = 2/3$, is a good approximation for this case. For epitope mapping, three kinds of FRET measurements were conducted on JY cells: 1) intramolecular FRET between donor-L368 and acceptor-W6/32 (R_3 distance), 2) intermolecular FRET between donor-W6/32 and acceptor-W6/32 (R_4 distance), and 3) intermolecular FRET between donor-L368 and acceptor-L368 (not indicated on Fig. 1*A*).

The FRET efficiency histograms constructed from cell by cell flow cytometric measurements (Fig. 1*B*) show that the distribution of intramolecular FRET efficiency (distances between the heavy and light chain epitopes on the same HLA molecule) is narrower than the distribution of intermolecular FRET efficiencies. This reflects that the homo-association (oligomerization) of class I HLA molecules is only partial, and also shows a heterogeneity over the cell population. The FRET efficiency data (means of the histograms) were converted to molecular distances, as described in the legends to Table I. The intramolecular epitope distance between β_2m (L368) and the heavy chain (W6/32) was ~6.8 nm, and the average distance between heavy chain epitopes (W6/32) of two neighboring HLA molecules was maximum 7.6 nm. The average distance between two neighboring light chain epitopes was a bit higher, 7.9 nm (Table I). These approximate molecular distances, considered as average distances between the mass centers of the V regions of Fab molecules, were used further on in the computer modeling, in which the error arising from the uncertainty of dye localization within the V (V_H and V_L) domains of Fab was also taken into account.

Mapping of the vertical distances of heavy and light chain epitopes from the surface of the plasma membrane by FRET

The relative position of class I HLA molecule to the exofacial surface of the plasma membrane has been estimated by FRET measurements between the heavy chain or the β_2m epitopes of the molecule labeled by fluorescent Fabs and a fluorescent phosphatidylcholine analogue, BODIPY-PC, localized in the polar, head group (surface) region of the plasma membrane. The BODIPY-PC molecules, however, may form a multiple acceptor array around donor Fab-labeled HLA molecules in the plane of the membrane, depending on their concentration. Thus, in this study, the actual acceptor density may also largely influence the FRET efficiency (29, 30). Therefore, in this case, FRET measurements were conducted at different donor/acceptor ratios (Fig. 1*C*). The FRET efficiencies were analyzed in terms of distances of closest approach from the Stern-Volmer plots of fluorescence quenching (Fig. 1*C*), according to Yguerabide (30) (see legend to Table I). The light chain (L368) epitope had a closest approach distance (R_2, Fig. 1*A*) of 7.5 ± 0.2 nm from the membrane surface, while the heavy chain (W6/32) epitope was found to be located closer (R_1: 6.2 ± 0.2 nm). In the further molecular modeling, these distance estimates, measured on intact live cells, were used in steric positioning of the x-ray-resolved HLA-A2 structures relative to the exofacial surface of the plasma membrane.

Docking of Fab to the crystallographic structure of HLA-A2

Fig. 2, *A* and *B*, demonstrates a model of the docking of fluorescent Fabs during the labeling procedure by selected amino acid residues in their hypervariable regions to the antigenic epitopes on the β_2m and heavy chain domains of the class I HLA molecule. A crystal structure of human Fab B7-15A2 (PDB code: 1AQK) was used as a model of W6/32 and L368 Fabs (see *Materials and Methods*). The relative positions of the geometrical centers of their V domains have been set to match the distances estimated from FRET measurements using donor- and acceptor-labeled Fabs (Table I).

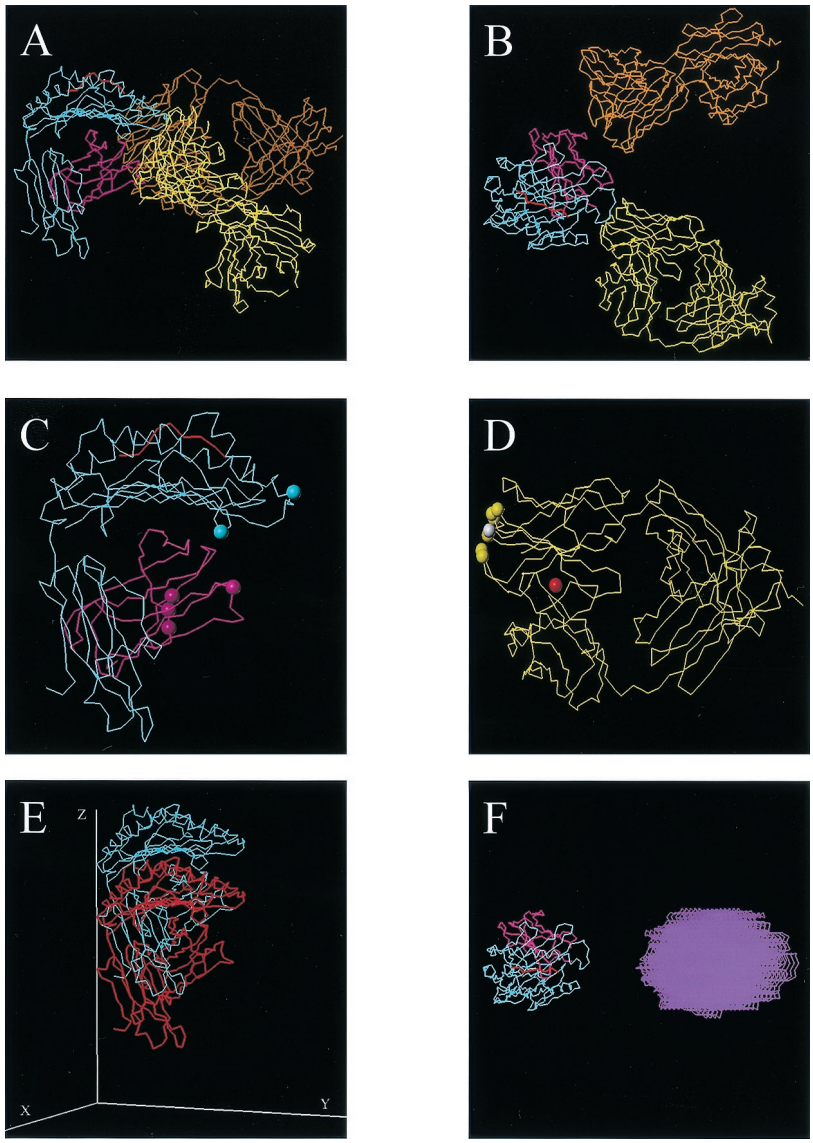

FIGURE 2. Molecular modeling procedure for locating 3D dimeric models of fluorescently labeled HLA-A2 molecules on the cell surface. Docking of fluorescence-labeled Fabs in yellow and orange colors is shown to the heavy chain (cyan) and to the β_2m domains (magenta) of the HLA-A2 molecule, respectively; *A*, perspective view above the plasma membrane; *B*, top view parallel to the plasma membrane. Amino acid residues of the HLA-A2 and Fab molecules involved in the specific HLA-Fab interaction are emphasized with spheres in *C* and *D*, respectively. The red dot in *D* points out the geometrical center of the V region of the Fab that has been used as the reference point for distance measurements. *E*, Vertical positioning of the HLA class I molecules above the plane of the plasma membrane (intramembrane segment of the molecule is not shown due to the lack of its crystallographic structure). Only the extreme positions are shown, closest to the plasma membrane (red), and farthest (cyan). *F*, Horizontally, HLA I molecules take up a relatively well-defined position with an equilibrium conformation in their dimeric complexes. The error limits of the procedure can be judged from *F*. Displayed configurations are results of molecular modeling based on 3D molecular arrangements similar to *A* and *B*.

The coordinate system is fixed to the plasma membrane surface (not shown).

The positions of the labels were confined to the geometrical center of V domain of the Fab molecules (red dot in Fig. 2*D*), since the Fabs seemed to be labeled preferentially at the same lysyl residue at 1:1 dye:Fab ratio, shown by sequencing and mass-spectrometric analysis of fragmented Abs conjugated with fluorescent dyes (Tőzsér et al., unpublished data). The high reproducibility of our FRET efficiency data obtained with independently labeled Fabs also confirms this observation. The Fab molecules are undergoing a restricted rotation around their binding sites in a cone fashion; therefore, the positions of the Fab molecules can be regarded as dynamic motional averages (34). The possible positions of the fluorescent Fabs relative to the class I HLA molecule have been determined by an automated screening procedure, as described above, throughout molecular modeling.

3D molecular models of dimeric and tetrameric forms of HLA-A2

The mean FRET efficiency measured between HLA molecules on JY B cells (and also on a number of transformed human B and T cell lines by Matkó et al. (12, 13)) ranges from 15 to 30%, indicating that a significant portion of HLA-I molecules is present in multimeric forms (e.g., dimers, trimers, tetramers, or higher oligomers) at the cell surface. FRET data alone are not able to precisely measure the extent of oligomerization or the fractional amount of different multimers, but clearly indicate their existence, since purely monomeric form of HLA class I at the cell surface is inconsistent with such an efficient FRET as measured in the present study. Accordingly, we searched for multimeric forms of the HLA class I molecules by molecular modeling.

Following the logic of pair-wise FRET measurements between different epitopes of the HLA class I molecule and also considering that free space must be allocated for fluorescent Fabs attached to both epitopes in a dimeric or higher order arrangement of HLA, an automated computer search sequence has been set up to find all possible relative positions of the two HLA class I molecules in their dimeric complex (for details of the procedure, see *Materials and Methods*). The identification for an allowed dimeric configuration was done by superimposing FRET-measured interepitope and epitope-cell surface distance data on the corresponding intermolecular distances in the 3D molecular modeling system. Intermolecular distances were measured in the 3D model between the geometrical centers of the V regions of the Fab molecules attached to the HLA class I epitopes and between those and the fluorescent dyes confined to the plane of the plasma membrane.

The first result of the above search procedure was the vertical localization of the HLA molecules in a 1.8-nm-thick layer above the plane of the plasma membrane, as displayed in Fig. 2*E*. Within this layer, one HLA class I molecule was fixed and used as reference, and the other molecule in the dimeric configuration was moved around in 0.2-nm steps, corresponding to the accuracy of the FRET measurements, and rotated around its vertical axis in a range of 0–360 degrees in 15-degree steps. Based on the above procedure, the distance between the two HLA class I molecules in their dimer is 7–9.4 nm, and the second molecule is rotated compared with the other in a range of −30 to +45 degrees. Fig. 2*F* nicely demonstrates the accuracy of the modeling procedure and shows that despite the relatively wide ranges of relative intermolecular distance and rotational angles, the HLA class I molecules are fairly well located in space. The relatively large number of sterically allowed dimeric configurations is consistent with the assumption that these dimers are not rigid entities, but they represent a dynamical molecular assembly embedded in the plasma membrane.

As a result of the above-described search procedure for sterically allowed and FRET- supported dimeric configurations, a representative sample was selected for further examination (Fig. 3, *A* and *B*). Fig. 3, *C* and *D*, shows another sterically allowed dimeric configuration, in which the class I HLA monomers labeled with both heavy chain- and β_2m-bound fluorescent Fabs can get to close proximity of each other. This 3D model of the dimeric configuration has been constructed on separate grounds from the one described previously (in Fig. 3, *A* and *B*). In this study, an analogy to the hypothetical model of cooligomerization of CD4, class II MHC, and TCR (37, 38) was assumed. In this case, the estimated distance between the fluorescent labels is far beyond the upper limit of the FRET measurements regardless of their exact position on the Fab molecules. Therefore, such arrangements can practically be excluded at physiological conditions.

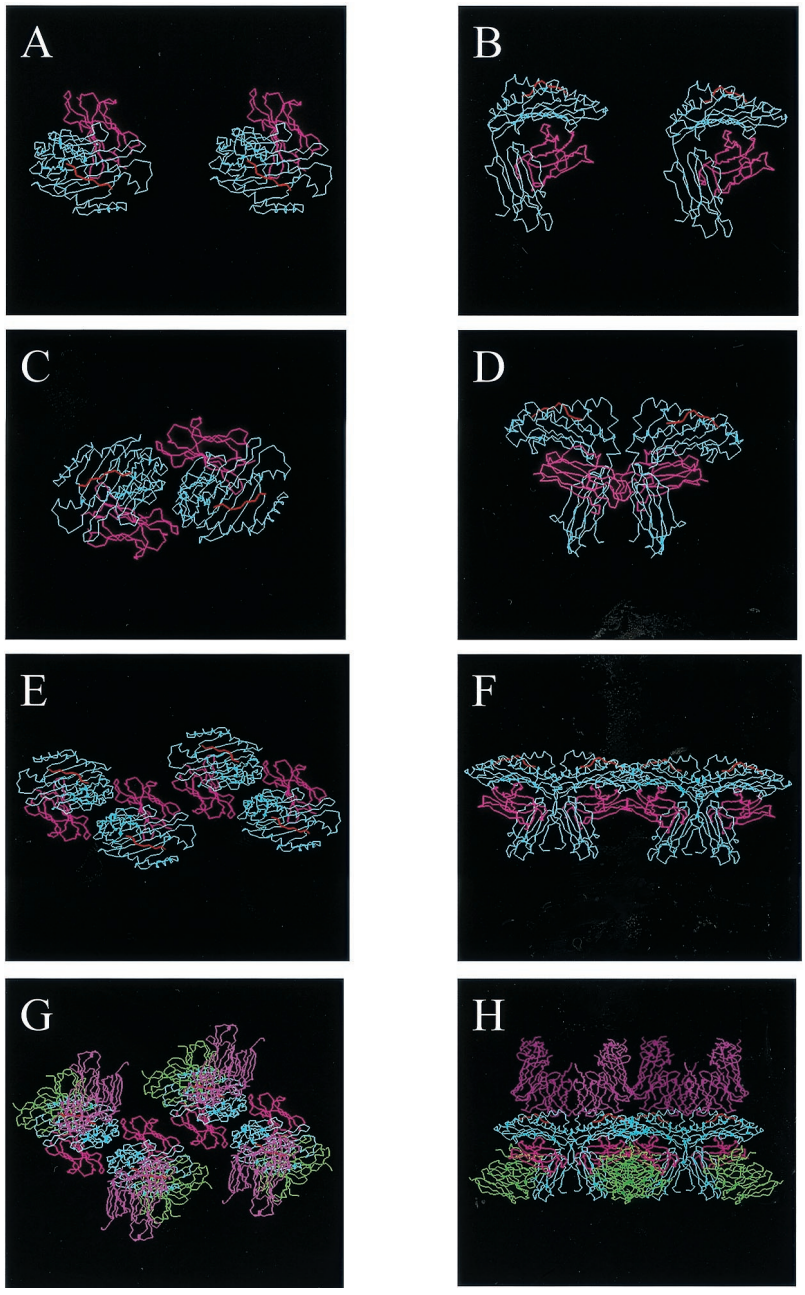

FIGURE 3. Possible molecular arrangements of class I HLA molecules in their dimeric (*A–D*) and tetrameric (*E*, *F*) homo-associates and the suggested model (*G*, *H*) of cooligomerization of dimeric CD8 (green), HLA class I, and TCR (purple) based on FRET-defined intermolecular distances and crystallographic structural data. The *left panels* show always top views, the *right ones* side views of the arrangements. The tetrameric configuration is a result of molecular modeling using the dimeric arrangements of *A* and *B* and *C* and *D*. Cooligomerization model (*G*, *H*) can serve as a functionally significant unit for a network of CD8-class I HLA multimolecular complexes to concentrate and cross-link the TCR with its associated signal transduction components at the site of the T cell-APC interface. Coloring scheme otherwise corresponds to that of Fig. 2.

We found that the elements of the previous two dimeric models can be used in combination to generate a likely tetrameric arrangement. Fig. 3, *E* and *F*, shows the 3D configuration of a class I HLA tetramer serving as reference points for FRET measurements. In this model of tetrameric molecular complex, the two external HLA molecules can bind both types of Fabs simultaneously, while the other two HLA can bind only anti-heavy chain Fab (W6/32), if one takes into account the steric limitations enforced by the two Fabs binding to the class I HLA molecule (see Fig. 2*B*). In this sterically allowed tetrameric configuration, an efficient FRET signal is expected between W6/32 and L368 Fabs attached to the same monomer and between two W6/32 Fabs attached to two different monomers, while no FRET is expected between two L368 Fabs attached to different monomers. This configuration matches well FRET data, as described in the discussion section. The lack of Fab on two of the four β_2m molecules is justified by the steric hindrance.

Fig. 3, *G* and *H*, represents a 3D model of cooligomerization of CD8, class I HLA, and the TCR molecules. This hypothetical model is based on FRET-defined intermolecular distances and crystallographic structural data, and uses the model of tetrameric arrangement of class I HLA molecules (Fig. 3, *E* and *F*). It was constructed by considering the structural features of contact sites reported for the HLA-A2-TCR complex (39) and for MHC-CD8 interaction (20, 40). This model represents a possible 3D organization of a multimolecular complex consistent with the present FRET data, the former x-ray crystallographic structures, and signal transduction studies on triggering of T cell activation (4). This structural arrangement can also serve as a functionally significant unit to form a network of CD8-class I HLA multimolecular complexes to concentrate and clusterize the TCR with its associated signal transduction components at the site of the T cell-APC interface. This might be especially important at low level of MHC-peptide challenge.

Discussion

Although sufficiently well-resolved x-ray structural models are available now for MHC, TCR, and the CD4 and CD8 coreceptor molecules and their complexes, the way that these molecules are organized at the surface of live cells (and at the target cell-effector cell contact region) into supramolecular complexes is still not fully understood. The 3D x-ray crystallographic structures derived from the extracellular domain of cell surface class I HLA do not account for their steric positioning (orientation) relative to the plane of the plasma membrane. The membrane-spanning α-helical segment of the HLA molecule and interactions with neighboring molecules can tilt or displace the extracellular domain of class I HLA molecules relative to the membrane surface.

With the help of the present, novel molecular modeling approach, we fitted the available x-ray structure of HLA-A2 molecules to in situ biophysical proximity data measured on live cells. The basic goal of the present computer-modeling work was to test whether sterically allowed dimeric and tetrameric arrangements of 3D HLA-A2 structures could be fitted to the FRET-based lateral and vertical epitope-mapping data measured on live cells.

The modeling was based on the following experimental data. Structural details of the HLA-A2 molecule have been studied by x-ray crystallography, and the structure of its complex with CD8 has recently been described (20). Antigenic epitopes, defined by mAbs L368 and W6/32, used in FRET measurements, have been localized on the β_2m and heavy chain domains of class I HLA molecule, respectively (31, 32). Binding domains of the contact area in the CD8$\alpha\alpha$-MHC complex have also been identified (40). The above information plus data from a FRET-based vertical distance mapping of HLA-I heavy and light chain epitopes from the surface of the plasma membrane of B cells, as well as data reporting on oligomeric forms of HLA-I on the cell surface, were all considered throughout the molecular modeling.

The modeling approach resulted in several 3D models of possible dimeric and tetrameric arrangements of class I HLA molecules matching well the FRET data measured on the surface of APCs (Fig. 3). A further advantage of the combined FRET-crystallographic structural modeling approach was pointed out by the possibility of positioning the Fab-binding epitopes on the light (β_2m) or heavy chains relative to the membrane surface, as demonstrated by Fig. 2, *A* and *B*. According to the crystallographic model of HLA-A2, the position of the β_2m was expected to be more membrane proximal because it was attached to the α_3-domain of the heavy chain. However, FRET data clearly showed that the Fab bound to the L368 epitope was located farther from the plane of the membrane than the Fab binding to the W6/32 epitope on the heavy chain.

Regarding the dimer models, a relatively large number of sterically allowed configurations could be constructed from molecular associations of class I HLA and Fab molecules similar to the one shown on Fig. 2, *A* and *B* (see Fig. 2*F*). These configurations, however, were based on the assumption of random orientation of monomeric units in the dimers after collisions limited by the lateral and rotational motional freedom of cell surface HLA-I molecules (41). However, by choosing the equilibrium distance and rotational angle as defined in the modeling procedure and allowing for the binding of both L368 and W6/32 Fabs, the number of possible, sterically, and FRET-allowed dimeric configurations could be reduced to one due to the steric constraints introduced by the bound Fabs (see model in Fig. 3, *A* and *B*). The other dimeric configuration shown on Fig. 3, *C* and *D*, was constructed by supposing an analogy to the lattice model of class II HLA superdimers (37, 38). In this configuration, the two HLA molecules were closer to each other, and the docked Fabs were pointing apart from each other (compare to Fig. 2*B*); thereby, the fluorescent labels were located far beyond the maximal distance probed by FRET. Therefore, the contribution of this configuration to the cell surface dimeric class I HLA population must be small, because the highly efficient FRET observed contradicts the large interepitope distance predicted in this study by the 3D molecular modeling.

The hypothetical, sterically allowed model proposed for HLA-I tetramers (Fig. 3, *E* and *F*), constructed from the two kinds of dimeric configurations, was consistent with a number of experimental observations on live B cells. 1) The mean intermolecular FRET efficiency between two anti-heavy chain Fabs was consistently higher than between two anti-β_2m Fabs. 2) A systematically lower number of binding sites was found on these (and also on other) cells for L368 Fab than for W6/32 Fab using a flow cytometric Scatchard analysis (see in Ref. 14), consistent with a possible shielding of L368 Fab binding site in a tetrameric (or higher oligomeric) arrangement. 3) Surprisingly, the efficiencies of intramolecular FRET between the β_2m (L368) and heavy chain (W6/32) epitopes were different in the opposite directions. If the donor label was located on L368, the FRET efficiency was consistently higher (33.0 $\pm$ 1.5%) than in the other direction, when the donor dye was on the W6/32 Fab (26.4 $\pm$ 2.2%). Since the distance of these epitopes was fixed within a monomeric unit, the same FRET efficiency was expected in either direction. Indeed, this might be the case for monomeric and dimeric forms of HLA-I molecules. However, assuming existence of tetramers corresponding to the model in Fig. 3, *E* and *F*, the situation is different. When L368 Fab carries the donor dye, there is always a proximal acceptor-labeled W6/32 Fab within the FRET distance (~10 nm), while if the donor dye is on the W6/32 Fab, only a part of the W6/32 Fabs could

contribute to FRET, because another part did not have acceptor-L368 Fab within the FRET-measuring range. Thus, a part of donor-W6/32 Fabs would contribute to FRET with the same efficiency as do the donor-L368 Fabs toward acceptor-W6/32 Fabs, while the rest would contribute with zero efficiency. Therefore, from the measured FRET efficiency values one could even estimate the maximal possible fraction of tetramers among the cell surface MHC-I molecules using the following train of thoughts. The lower FRET efficiency (26.4%) is consistent with a picture in which 80% of donor-W6/32 Fabs participated in FRET, while 20% did not. Since in the tetramer two of the four β_2m still can bind L368 Fab, we could say that at most 40% of the total cell surface β_2m is located in tetrameric forms, while at least 60% of β_2m exists in monomeric or dimeric forms. If higher oligomers ($n > 4$) were also present, then on the basis of FRET data we could say that the monomers and dimers together had larger proportions than 60% of the total class I HLA molecules.

Earlier x-ray data directly revealed superdimers of class II HLA molecules, but failed to predict such structures for class I HLA molecules to date. In contrast, a large number of physical measurements on proximity (by FRET), rotational and lateral mobility, and cell surface distribution (by scanning near-field optical microsopy) of HLA-I strongly indicated the existence of such supramolecular structures in the plasma membrane of live human cells (10, 12–15, 42, 43). Our FRET data measured on JY B cells were also in good accordance with these observations. Thus, the 3D models presented in this work could be considered as highly likely supramolecular structures formed from HLA-I molecules at the surface of potential APCs. Besides the momoneric, dimeric, trimeric, and tetrameric forms, larger clusters ($n > 4$) might also exist on the cell surface, as indicated by rotational mobility (42) and scanning near-field optical microscopy (43) data. Such clusters were supposed to be initiated and/or stabilized by β_2m-free heavy chains (12, 44, 45).

These oligomeric structures may have functional significance, as well. Using agonist and partial antagonist peptide-loaded soluble murine class I MHC (E^k) and soluble TCR, Reich et al. (46) reported on a ligand-specific oligomerization of TCR in solution. Moreover, using soluble monomers, dimers, trimers, and tetramers of class I MHC (E^k) ligands to stimulate intact T cells, they found the monomers of agonist peptide-loaded MHC nonstimulatory, the dimers weakly stimulatory, while the trimers or tetramers proved to be highly potent stimuli (5). These observations support the likeliness of a ligand-driven TCR clustering through multivalent engagement, also proposed earlier for human cells (12). Our models based also on in situ physical measurements underline the reality of such multivalent engagement. Such HLA-I oligomers may also appear in the contact areas of APC-T cell conjugates serving as key elements of immunological synopses (3, 47, 48).

Conflicting data and theories have been reported about the necessary triggering threshold of T cell activation with respect to the necessary number of HLA-peptide ligands. Delon et al. (4) demonstrated that soluble monomers of murine MHC-peptide complexes were able to trigger calcium signals, but only in $CD8^+$ T cells. It was also demonstrated that CD8 molecules could increase the apparent affinity of MHC-peptide ligands for the TCR (49, 50). Earlier works definitely supported the close cooperation and molecular proximity of peptide-MHC and CD8 (51), also at the interface of target and effector cells probed directly by intercellular FRET measurements between Ag-presenting and effector cells (47). Considering the CD8-class I HLA interaction, the present model of HLA tetramer was further expanded with the 3D structural entities of the connecting CD8 and TCR molecules. A multimolecular complex involving the molecular entities of dimeric CD8, class I HLA, and the TCR could directly be generated from the above tetrameric HLA model without any steric hindrance (see Fig. 3, *G* and *H*). Such supramolecular assembly of class I HLA oligomers with CD8 molecules and TCRs can be considered as a possible protein cluster existing in Ag-presenting-effector cell conjugates and comprising several functional advantages: 1) the possibility of multivalent engagement of TCRs; 2) TCR clustering may be promoted by the supramolecular complex displayed in Fig. 3, *E* and *F* or its expanded CD8/MHC-peptide network; 3) these multimolecular clusters together with other accessory molecules (e.g., adhesion proteins) may also promote formation of an immunological synapse (48) at the contact site.

In conclusion, the newly introduced computer-modeling approach based on the combination of x-ray-resolved 3D structures and in situ FRET data measured on live cells offers the advantage of constructing realistic 3D structural models of supramolecular protein complexes in the plasma membrane of cells. By expanding the 3D model of HLA-I oligomers via connecting CD8 dimers and TCRs to it, the existence of a supramolecular complex is predicted that may contribute with an enhanced efficiency to T cell stimulation by multivalent engagement/clustering of TCRs with a cooperating CD8 molecule essential to initialize T cell signaling. This model is compatible with the data of both Boniface et al. (5) and Delon et al. (4); thus, it can partly resolve their apparent contradiction, especially at low level of MHC-peptide stimulus. Similarly, T cell activation threshold has been found recently to depend on the oligomerization degree of chemically defined MHC class II oligomers (52). The presented 3D models are in good accordance with the results of in situ physical measurements of HLA-I distribution/proximity and mobility on live cells. Although throughout this work B cells and not professional APCs (e.g., dendritic cells) were used, we believe that our models help to understand the yet unclear principles of molecular organization of Ag-presenting MHC molecules on the surface of APCs. The present physical analysis can be further extended to APC-CTL conjugates where these molecules are in situ interacting with TCRs and accessory molecules. With the growing number of available x-ray structures of important cell surface macromolecules, the applicability of the method can easily be extended to other significant questions of immunology.

Acknowledgments

We thank Z. Huang and coworkers for kindly providing coordinates of their CD4/MHC-II oligomerization model.

References

1. Germain, R. N. 1997. T cell signaling: the importance of receptor clustering. *Curr. Biol. 7:R640.*
2. Lanzavecchia, A., G. Iezzi, and A. Viola. 1999. From TcR engagement to T cell activation: a kinetic view of T cell behavior. *Cell 96:1.*
3. Monks, C. R. F., B. A. Freiberg, H. Kupfer, N. Sciaky, and A. Kupfer. 1998. Three dimensional segregation of supramolecular activation clusters in T cells. *Nature 395:82.*
4. Delon, J., C. Gregoire, B. Malissen, S. Darche, F. Lemaitre, J. Kourilsky, P. Abastado, and A. Trautmann. 1998. CD8 expression allows T cell signaling by monomeric peptide-MHC complexes. *Immunity 9:467.*
5. Boniface, J. J., J. D. Rabinowitz, C. Wülfing, J. Hampl, Z. Reich, J. D. Altman, R. M. Kantor, C. Beeson, H. McConnell, and M. M. Davies. 1998. Initiation of signal transduction through the T-cell receptor requires the peptide multivalent engagement of MHC ligands. *Immunity 9:459.*
6. Damjanovich, S., J. Szöllősi, and L. Trón. 1992. Transmembrane signaling in lymphocytes. *Immunol. Today 13:A12.*
7. Damjanovich, S., R. Gáspár, Jr., and C. Pieri. 1997. Dynamic receptor superstructures at the plasma membrane. *Q. Rev. Biophys. 30:67.*
8. Matkó, J., and M. Edidin. 1997. Energy transfer methods for detecting molecular clusters on cell surfaces. *Methods Enzymol. 278:444.*
9. Jacobson, K., E. D. Sheets, and R. Simson. 1995. Revisiting the fluid mosaic model of membranes. *Science 268:1441.*
10. Smith, P. R., I. E. G. Morisson, K. M. Wilson, N. Fernandez, and R. J. Cherry. 1999. Anomalous diffusion of major histocompatibility complex class I molecules on HeLa cells determined by single particle tracking. *Biophys. J. 76:3331.*

11. Chakrabarti, A., J. Matkó, N. A. Rahman, B. G. Barisas, and M. Edidin. 1992. Self-association of class I major histocompatibility complex molecules in liposome and cell membranes. *Biochemistry 31:7182.*
12. Matkó, J., Y. Bushkin, T. Wei, and M. Edidin. 1994. Clustering of class I HLA molecules on the surfaces of activated and transformed human cells. *J. Immunol. 152:3353.*
13. Matkó, J., A. Jenei, T. Wei, and M. Edidin. 1995. Luminescence quenching by long range electron transfer: a probe of protein clustering and conformation at the cell surface. *Cytometry 19:191.*
14. Bene, L., M. Balázs, J. Matkó, J. Möst, M. Dierich, J. Szöllősi, and S. Damjanovich. 1994. Lateral organization of the ICAM-1 molecule at the surface of human lymphoblasts: a possible model for its co-distribution with the IL-2 receptor, class I and class II HLA molecules. *Eur. J. Immunol. 24:2115.*
15. Szöllősi, J., L. Bene, V. Horejsi, P. Angelisova, and S. Damjanovich. 1996. Supramolecular complexes of MHC class I, MHC class II, CD20, and tetraspan molecules (CD53, CD81, and CD82) at the surface of a B cell line JY. *J. Immunol. 157:2939.*
16. Jenei, A., S. Varga, L. Bene, L. Mátyus, A. Bodnár, Zs. Bacsó, C. Pieri, R. Gáspár, Jr., T. Farkas, and S. Damjanovich. 1997. HLA class I and II antigens are partially co-clustered in the plasma membrane of human lymphoblastoid cells. *Proc. Natl. Acad. Sci. USA 94:7269.*
17. Bjorkman, P. J., M. A. Saper, B. Samraoui, W. S. Bennett, J. L. Strominger, and D. C. Wiley. 1987. Structure of the human class I histocompatibility antigen HLA-A2. *Nature 329:506.*
18. Guo, H.-C., T. S. Jardetzky, T. P. J. Garrett, W. S. Lane, J. L. Strominger, and D. C. Wiley. 1992. Different length peptides bind to HLA-Aw68 similarly at their ends but bulge out in the middle. *Nature 360:364.*
19. Brown, J. H., T. S. Jardetzky, J. C. Gorga, L. J. Stern, R. G. Urban, J. L. Strominger, and D. C. Wiley. 1993. Three-dimensional structure of human class II histocompatibility antigen HLA-DR1. *Nature 364:33.*
20. Gao, F. G., J. Tormo, U. C. Gerth, J. R. Wyer, A. J. McMichael, D. I. Stuart, J. I. Bell, E. Y. Jones, and B. K. Jakobsen. 1997. Crystal structure of the complex between human CD8$\alpha\alpha$ and HLA-A2. *Nature 387:630.*
21. Terhorst, C., P. Parham, D. L. Mann, and J. L. Strominger. 1976. Structure of HLA antigens: amino acid and carbohydrate compositions and NH2-terminal sequences of four antigen preparations. *Proc. Natl. Acad. Sci. USA 73:910.*
22. Edidin, M., and T. Wei. 1992. Lateral diffusion of H-2 antigens on mouse fibroblasts. *J. Cell Biol. 95:458.*
23. Bassi, G. S., A. I. Murchie, T. Walter, R. M. Clegg, and D. M. Lilley. 1997. Ion-induced folding of the hammerhead ribozyme: a fluorescence resonance energy transfer study. *EMBO J. 16:7481.*
24. Bene, L., J. Szöllősi, M. Balázs, L. Mátyus, R. Gáspár, Jr., M. Ameloot, R. E. Dale, and S. Damjanovich. 1997. Major histocompatibility complex class I protein conformation altered by transmembrane potential changes. *Cytometry 27: 353.*
25. Szöllősi, J., L. Trón, S. Damjanovich, S. H. Helliwell, D. J. Arndt-Jovin, and T. M. Jovin. 1984. Fluorescence energy transfer measurements on cell surfaces: a critical comparison of steady state fluorimetric and flow cytometric methods. *Cytometry 5:210.*
26. Trón, L., J. Szöllősi, S. Damjanovich, S. H. Helliwell, D. J. Arndt-Jovin, and T. M. Jovin. 1984. Flow cytometric measurements of fluorescence resonance energy transfer on cell surfaces: quantitative evaluation of the transfer efficiency on a cell-by-cell basis. *Biophys. J. 45:939.*
27. Matkó, J., J. Szöllősi, L. Trón, and S. Damjanovich. 1988. Luminescence spectroscopic approaches of cell surface dynamics. *Q. Rev. Biophys. 21:479.*
28. Szöllősi, J., L. Mátyus, L. Trón, M. Balázs, I. Ember, M. J. Fulwyler, and S. Damjanovich. 1987. Flow cytometric measurements of fluorescence energy transfer using single laser excitation. *Cytometry 8:120.*
29. Valenzuela, C. F. P. Weign, J. Iquerabide, and D. A. Johnson. 1994. Transverse distance between the membrane and the agonist binding sites on the *Torpedo* acetylcholine receptor: a fluorescence study. *Biophys. J. 66:674.*
30. Yguerabide, J. 1994. Theory for establishing proximity relations in biological membranes by excitation energy transfer measurements. *Biophys. J. 66:683.*
31. Smith, K. D., Z. B. Kutago, and C. T. Lutz. 1997. Conformational changes in MHC class I molecules. *Immunol. Res. 16:243.*
32. Trymbulak, W. P., and R. A. Zeff. 1997. Mutants of human β_2-microglobulin map and immunodominant epitope within the three-stranded β-pleated sheet. *Transplantation 64:640.*
33. Ladasky, J. J., B. P. Shum, F. Canavez, H. N. Seuánez, and P. Parham. 1999. Residue three of β_2-microglobulin affects binding of class I MHC molecules by the W6/32 antibody. *Immunogenetics 49:312.*
34. Kubitscheck, U., R. Schweitzer-Stenner, D. J. Arndt-Jovin, T. M. Jovin, and I. Pecht. 1993. Distribution of type I Fcϵ-receptors on the surface of mast cells probed by fluorescence resonance energy transfer. *Biophys. J. 64:110.*
35. Thompson, J. D., D. G. Higgins, and T. J. Gibson. 1994. CLUSTAL W: improving the sensitivity of progressive multiple sequence alignment through sequence weighting, positions-specific gap penalties and weight matrix choice. *Nucleic Acids Res. 22:4673.*
36. Dale, R. E., J. Eisinger, and W. E. Blumberg. 1979. The orientational freedom of molecular probes: the orientation factor in intramolecular energy transfer. *Biophys. J. 26:161.*
37. Huang, Z., S. Li, and R. Korngold. 1997. Immunoglobulin superfamily proteins: structure, mechanisms, and drug discovery. *Biopolymers 43:367.*
38. Li, S., T. Satoh, R. Korngold, and Z. Huang. 1998. CD4 dimerization and oligomerization: implications for T-cell function and structure-based drug design. *Immunol. Today 19:455.*
39. Garboczi, D. N., P. Ghosh, U. Utz, Q. R. Fan, W. E. Biddison, and D. C. Wiley. 1996. Structure of the complex between human T cell receptor, viral peptide and HLA-A2. *Nature 384:134.*
40. Devine, L., J. Sun, M. R. Barr, and P. B. Kavathas. 1999. Orientation of the Ig domains of CD8$\alpha\beta$ relative to MHC class I. *J. Immunol. 162:846.*
41. Edidin, M. 1988. Function by association? MHC antigens and membrane receptor complexes. *Immunol. Today 9:218.*
42. Damjanovich, S., G. Vereb, A. Shaper, A. Jenei, J. Matkó, J. P. P. Starink, G. O. Fox, D. J. Arndt-Jovin, and T. M. Jovin. 1995. Structural hierarchy in the clustering of HLA class I molecules in the plasma membrane of human lymphoblastoid cells. *Proc. Natl. Acad. Sci. USA 92:1122.*
43. Hwang, J., L. A. Gheber, L. Margolis, and M. Edidin. 1998. Domains in cell plasma membranes investigated by near-field scanning optical microscopy. *Biophys. J. 74:2184.*
44. Demaria, S., and Y. Bushkin. 1993. CD8 and β_2-microglobulin-free MHC class I molecules in T cell immunoregulation. *Int. J. Clin. Lab. Res. 23:61.*
45. Carreno, B. M., and T. H. Hansen. 1994. Exogenous peptide ligand influences the expression and half-life of free HLA class I heavy chains ubiquitously detected at the cell surface. *Eur. J. Immunol. 24:1285.*
46. Reich, Z., J. J. Boniface, D. S. Lyons, N. Borochov, E. J. Wachtel, and M. M. Davis. 1997. Ligand-specific oligomerization of T cell receptor molecules. *Nature 387:617.*
47. Bacsó, Zs., L. Bene, A. Bodnár, J. Matkó, and S. Damjanovich. 1996. A photobleaching energy transfer analysis of CD8/MHC I and LFA/ICAM-1 interactions in CTL-target cell conjugates. *Immunol. Lett. 54:151.*
48. Dustin, M. L., and A. S. Show. 1999. Costimulation: building an immunological synapse. *Science 283:649.*
49. Luescher, I. F., E. Vivier, A. Layer, J. Mahiou, F. Godeau, B. Malissen, and P. Romero. 1995. CD8 modulation of T-cell antigen receptor-ligand interactions on living cytotoxic lymphocytes. *Nature 373:353.*
50. Kessler, B., D. Hudrisier, J.-C. Cerrotini, and I. F. Luescher. 1997. Role of CD8 in aberrant function of cytotoxic T lymphocytes. *J. Exp. Med. 182:779.*
51. Bushkin, Y., S. DeMaria, J. Le, and R. Schwab. 1988. Physical association between CD8 and HLA class I molecules on the surface of activated human T lymphocytes. *Proc. Natl. Acad. Sci. USA 85:3985.*
52. Cochran, J. R., T. O. Cameron, and L. J. Stern. 2000. The relationship of MHC-peptide binding and T cell activation probed using chemically defined MHC class II oligomers. *Immunity 12:241.*